THE JOURNAL OF PHYSICAL CHEMISTRY A

Article

pubs.acs.org/JPCA

Photoelectron Spectroscopy and *ab initio* Calculations of $Li(H_2O)_n^-$ and $Cs(H_2O)_n^-$ (n = 1−6) Clusters

Zhen Zeng,[†] Cheng-Wen Liu,[‡] Gao-Lei Hou,[†] Gang Feng,[†] Hong-Guang Xu,[†] Yi Qin Gao,*[,‡] and Wei-Jun Zheng*[,†]

[†]Beijing National Laboratory for Molecular Sciences, State Key Laboratory of Molecular Reaction Dynamics, Institute of Chemistry, Chinese Academy of Sciences, Beijing 100190, China

[‡]Beijing National Laboratory for Molecular Sciences, Institute of Theoretical and Computational Chemistry, College of Chemistry and Molecular Engineering, Peking University, Beijing 100871, China

Supporting Information

ABSTRACT: The $Li(H_2O)_n^-$ and $Cs(H_2O)_n^-$ (n = 0−6) clusters were studied using anion photoelectron spectroscopy combined with *ab initio* calculations. It was found that Li tends to be surrounded by water molecules with no water−water H-bonds being formed in the first hydration shell; while Cs sticks on the surface of water−water H-bonds network. The Li atom in its anionic or neutral state is surrounded by four water molecules through Li−O interactions within the first hydration shell; while the case of Cs is different. For the anionic $Cs(H_2O)_n^-$ clusters, two types of structures, namely H-end and O-end structures, were identified, with nearly degenerate energies. For the neutral $Cs(H_2O)_n$ clusters, only O-end structures exist and the first hydration shell of the Cs atom has four water molecules. The different hydration nature of Li and Cs atoms can be ascribed to the delicate balance between the alkali metal−water interactions and the water−water interactions as well as the effect of excess electron.

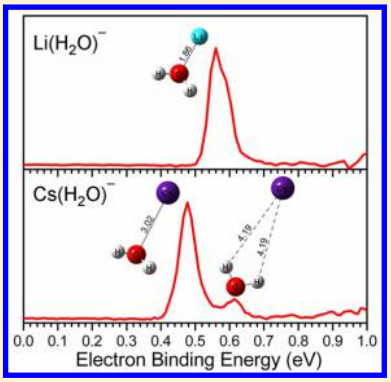

1. INTRODUCTION

Hydration of alkali metals is a fundamental process which has attracted considerable research interests in the fields of inorganic chemistry, biochemistry, and computational chemistry. Many studies were focused on the hydrated alkali metal cations aiming to investigate the alkali metal ion−water interactions with thermodynamic equilibrium measurements,[1−3] in which the equilibrium constants for the hydration reactions of alkali cations and the bond energies of water to alkali cations were determined. The infrared photodissociation spectroscopy[4−9] experiments were carried out to gain the geometric information about the hydrated alkali cations. A number of theoretical calculations[10−22] were conducted to shed light on the hydrated alkali cations in terms of structures, thermodynamic properties as well as IR frequencies.

For hydrated alkali atoms, the pioneering studies were the photoionization threshold measurements of $Na(H_2O)_n$,[23−25] $Cs(H_2O)_n$[26] and $Li(H_2O)_n$.[27] It has been found that the ionization potentials of $Li(H_2O)_n$, $Na(H_2O)_n$, and $Cs(H_2O)_n$ all rapidly decrease with increasing number of water molecules and converge to the vertical detachment energy (VDE) of the hydrated electron in liquid water (3.2 eV)[28] at n = 4. These processes relate to the solvated electron and are mainly identified in terms of transformation from one-center Rydberg-like states to two-center ion pair states as suggested by theoretical investigations.[29−40] Recently, the $Na(H_2O)_{1-22}$ clusters were investigated using pump−probe femtosecond-laser experiment to study the dynamics of the first electronically excited state of solvated electron.[41]

Solvated electron pairs play key roles in many biochemical processes.[42−44] It has been suggested that hydrated alkali anions such as $Li(H_2O)_n^-$ and $Na(H_2O)_n^-$ may serve as gas-phase molecular models for the solvation of two electrons which is important for understanding the electron−electron interaction in solution.[45] The different electron pair distribution was theoretically analyzed for $Li(H_2O)_n^-$ and $Na(H_2O)_n^-$, in which a solvated electron pair detached from the Li atom is present in $Li(H_2O)_{10}^-$, while two electrons stay on the Na atom, owing to their different structures with Na^- sticking on the cluster surface but Li being surrounded by water molecules.[45] Other theoretical studies were conducted to investigate the structures and the VDEs of $Li(H_2O)_n^-$ and $Na(H_2O)_n^-$ (n = 1−4).[46−48] Anion photoelectron spectroscopy[27,49] and vibrational absorption spectroscopy[50−53] were carried out to get further insight into the electronic and geometric structures. The photoelectron spectroscopy results on $Li(D_2O)_n^-$[49] and $Na(H_2O)_n^-$[27] exhibited different spectral shift with n up to 4 due to the variation in the solute−solvent interaction energy.

To further understand the hydration of alkali atoms at the molecular level, here we investigated the size dependence of the

Received: December 7, 2014
Revised: February 26, 2015
Published: February 27, 2015

DOI: 10.1021/jp512177j
J. Phys. Chem. A 2015, 119, 2845−2856

electronic structures and coordination geometries of alkali metal−water clusters using mass-selected anion photoelectron spectroscopy and *ab initio* calculations. $Li(H_2O)_n^-$ and $Cs(H_2O)_n^-$ (n = 0−6) were chosen as the model systems considering their distinct atom radii and surface charge densities.

2. EXPERIMENTAL AND COMPUTATIONAL METHODS

2.1. Experimental Methods. The experiments were conducted on a home-built apparatus consisting of a time-of-flight mass spectrometer and a magnetic-bottle photoelectron spectrometer, which has been described previously.[54] Briefly, the $Li(H_2O)_n^-$ and $Cs(H_2O)_n^-$ clusters were produced in a laser vaporization source by ablating rotating and translating LiI or CsI disc targets with the second harmonic (532 nm) light pulses of the Nd: YAG laser, while helium carrier gas with ∼4 atm backing pressure seeded with water vapor was allowed to expand through a pulsed valve for generating hydrated alkali metal anions and cooling the formed clusters. The cluster anions were mass-analyzed by the time-of-flight mass spectrometer. The $Li(H_2O)_n^-$ and $Cs(H_2O)_n^-$ (n = 0−6) clusters were each mass-selected and decelerated before being photodetached by another Nd: YAG laser. The photodetached electrons were collected and energy-analyzed by the magnetic-bottle photoelectron spectrometer. The photoelectron spectra were calibrated using the spectra of Li^-, Cs^-, and Bi^- taken at similar conditions. The instrumental resolution was ∼40 meV for electrons with 1 eV kinetic energy.

2.2. Computational Methods. The Gaussian09[55] program package was used for all the calculations. The structures of $Li(H_2O)_n^-$ and $Cs(H_2O)_n^-$ (n = 1−6) clusters and their neutral counterparts were optimized using density functional theory employing the M06-2X functional.[56] We used the standard Pople-type basis set 6-311++G** for the Li, O, and H atoms. The effective core potential (ECP) basis set Def2-TZVPPD,[57] obtained from the EMSL basis set library,[58] was used for the Cs atom. Harmonic vibrational frequencies were calculated to make sure that the obtained structures are the real local minima. No symmetry constraint was employed during the optimizations. In order to obtain more accurate energies of $Li(H_2O)_n^-$ (n = 1−6) and the corresponding vertical detachment energies, single-point energy calculations were conducted using CCSD(T) method[59] with the same basis set. All the calculated energies except the VDEs have been corrected by the zero-point vibrational energies. To evaluate the chosen functional M06-2X, the $Li(H_2O)_n^-$ clusters and their corresponding neutrals were also calculated using other two variants of hybrid functionals, LC-ωPBE[60−63] and ωB97XD.[64] We found that the VDEs calculated by the M06-2X functional are in better agreement with the experimental values than those by the LC-ωPBE and ωB97XD functionals (see Supporting Information). Thus, the M06-2X functional is used in this work.

3. EXPERIMENTAL RESULTS

The photoelectron spectra of $Li(H_2O)_n^-$ (n = 0−6) clusters recorded with 1064 and 532 nm photons are presented in Figure 1, and those of $Cs(H_2O)_n^-$ (n = 0−6) are displayed in Figure 2. The VDEs and the adiabatic detachment energies (ADEs) of $Li(H_2O)_n^-$ and $Cs(H_2O)_n^-$ (n = 0−6) clusters estimated from their photoelectron spectra are summarized in Table 1. The VDEs were measured from the maxima of the corresponding peaks. Considering the broadening of the photoelectron spectra due to the instrumental resolution, the ADE was estimated by adding the value of the instrumental resolution to the electron binding energy (EBE) at the crossing point of the baseline and the leading edge of the first peak.

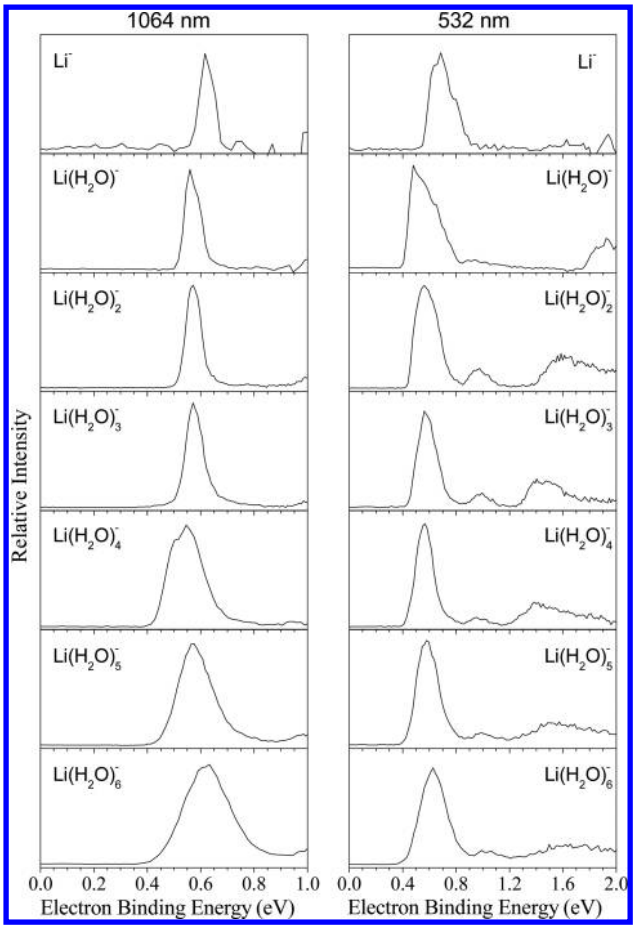

Figure 1. Photoelectron spectra of $Li(H_2O)_n^-$ (n = 0−6) recorded with 1064 and 532 nm photons.

In Figure 1, the 1064 and 532 nm spectra of Li^- display one feature centered at 0.62 eV, consistent with the experimental value (0.618 eV) of Pegg et al.[65] The 1064 nm spectrum of $Li(H_2O)^-$ exhibits a sharp peak centered at 0.56 eV, 0.06 eV lower than that of bare Li^-. A broad feature at around 1.90 eV shows up in the 532 nm spectrum, which can be assigned to the transition from the anion ground state to the first excited state of neutral. In the 1064 nm spectra of $Li(H_2O)_{2-3}^-$, the band position and width remain nearly constant at 0.57 eV. The 532 nm spectrum of $Li(H_2O)_2^-$ shows another band centered at 0.96 eV, higher than the main feature by 0.39 eV (3150 cm^{-1}), close to the O−H stretching of water molecules. The broad feature at around 1.60 eV can also be assigned to the transition to the first excited state of neutral, analogous to the case of $Li(H_2O)^-$. The 532 nm spectrum of $Li(H_2O)_3^-$ is similar to that of $Li(H_2O)_2^-$ with the spacing of 3310 cm^{-1} between the first two features. For $Li(H_2O)_4^-$, the major peak slightly shifts to the lower EBE of 0.55 eV and its width becomes wider than those of n = 0−3. The band centered at 0.96 eV and the broad feature at around 1.40 eV shown in the 532 nm spectrum of $Li(H_2O)_4^-$ can be attributed to the similar transitions as those of $Li(H_2O)_{2-3}^-$. The major features of $Li(H_2O)_5^-$ and $Li(H_2O)_6^-$ monotonically shift to the higher EBE again,

DOI: 10.1021/jp512177j
J. Phys. Chem. A 2015, 119, 2845−2856

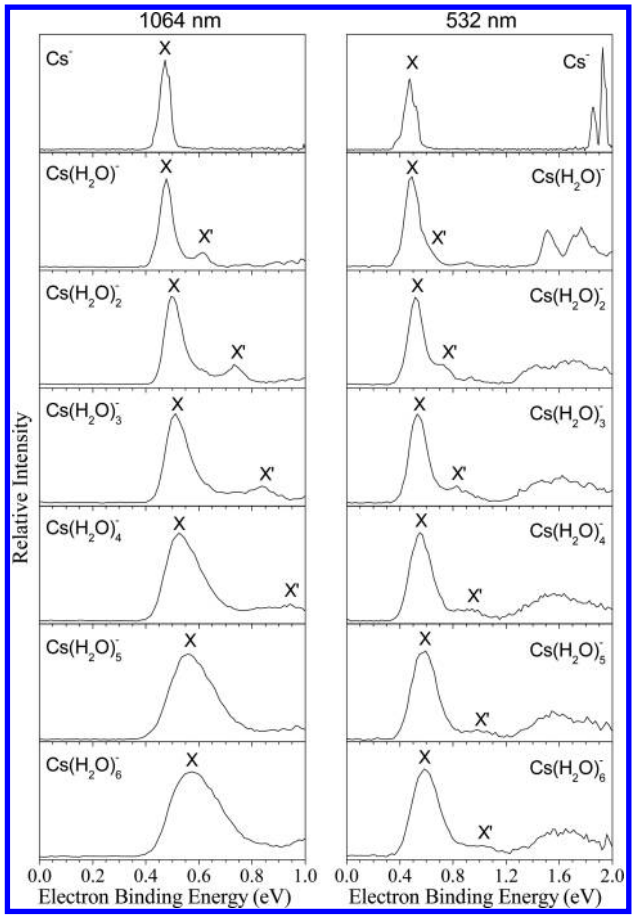

Figure 2. Photoelectron spectra of $Cs(H_2O)_n^-$ (n = 0–6) recorded with 1064 and 532 nm photons.

centered at 0.57 and 0.63 eV, respectively. The 532 nm spectra of $Li(H_2O)_5^-$ and $Li(H_2O)_6^-$ have the spectral patterns similar to those of $Li(H_2O)_{2-4}^-$. The spectral trend of $Li(H_2O)_n^-$ in this work is similar to that of $Li(D_2O)_n^-$.[49]

In Figure 2, the 1064 nm spectrum of Cs^- exhibits one feature at 0.47 eV and the 532 nm spectrum presents three bands centered at 0.47, 1.86, and 1.93 eV which can be assigned to the transitions from the Cs^- ground state to the ground, first and second excited states of Cs, respectively, in good agreement with the experimental results (0.47, 1.88, and 1.94 eV respectively) of Lineberger et al.[66] The 1064 nm spectrum of $Cs(H_2O)^-$ shows a major peak X at 0.48 eV, not shifting significantly with respect to that of bare Cs^-. There is a weak peak X′ centered at 0.61 eV, which can be tentatively assigned to a low-lying isomer. In the 532 nm spectrum of $Cs(H_2O)^-$, the other two features at higher EBE can be ascribed to the transitions to two excited states of neutral. The major features X of $Cs(H_2O)_2^-$, $Cs(H_2O)_3^-$, $Cs(H_2O)_4^-$, $Cs(H_2O)_5^-$, and $Cs(H_2O)_6^-$ are centered at 0.50, 0.51, 0.52, 0.56, and 0.57 eV, respectively, with the weak features X′ of those being at 0.73, 0.84, 0.94, 1.03, and 1.08 eV, respectively. As the number of water molecules increases, the main feature X shifts smoothly to the higher EBE with a broadened bandwidth, while the weak peak X′ shifts further to the higher EBE until it is only recorded by the 532 nm photons with a reduced intensity. In the spectra of $Cs(H_2O)_{2-6}^-$ recorded with 532 nm photons, there are also unresolved broad bands between 1.2 and 2.0 eV corresponding to the transitions from the anionic ground states to the excited states of neutrals.

4. THEORETICAL RESULTS AND DISCUSSION

The typical low-lying isomers of $Li(H_2O)_n^-$ and $Li(H_2O)_n$ (n = 1–6) are summarized in Figures 3 and 4, and those of $Cs(H_2O)_n^-$ and $Cs(H_2O)_n$ (n = 1–6) in Figures 5 and 6. More isomers are provided in the Supporting Information. We use labels of $(m + n)$ to identify the structures of $Li(H_2O)_n^{-/0}$, in which the m and n denote the number of water molecules in the first and second hydration shells, respectively. The relative energies, ADEs and VDEs of these low-lying isomers are summarized and compared with the experimental values in Tables 2 and 3.

4.1. $Li(H_2O)_n^-$ and $Li(H_2O)_n$. As shown in Figure 3, in the most stable isomer of $Li(H_2O)^-$ (1A), the water molecule is bound to the Li atom via its oxygen atom with a Li–O distance of 1.86 Å. The theoretical VDE of isomer 1A is 0.51 eV, in excellent agreement with the experimental value (0.56 eV). Isomer 1B has the water molecule interacting with Li via its two H atoms. It is less stable than 1A by 0.17 eV. Thus, we suggest that isomer 1A is the probable one contributing to the experimental spectrum. For neutral $Li(H_2O)$, the isomer (1a) in configuration similar to 1A is found to be the global minimum with almost unchanged Li–O bond length.

The lowest lying isomer of $Li(H_2O)_2^-$ (2A) has two water molecules symmetrically bonded to the Li atom with a nearly identical Li–O bond length in comparison with that of 1A. Its calculated VDE (0.51 eV) is in good accordance with the experimental value (0.57 eV). Considerably less energetically favorable isomer 2B is evolved from 1A with the second water molecule only forming hydrogen bond (H-bond) with the first one. Thus, isomer 2A is most likely to be present in our experiments. The structure of neutral isomer 2a is analogous to that of 2A but with different O–H bonds orientations. The symmetrical stretching of water molecules is calculated to be 3634 cm^{-1}, confirming the experimental observation of the 0.96 eV band.

Table 1. Experimentally Observed ADEs and VDEs of $Li(H_2O)_n^-$ and $Cs(H_2O)_n^-$ (n = 0–6) from Their Photoelectron Spectra

				X		X′	
cluster	ADE (eV)	VDE (eV)	cluster	ADE (eV)	VDE (eV)	ADE (eV)	VDE (eV)
Li^-	0.57	0.62	Cs^-	0.42	0.47		
$Li(H_2O)^-$	0.52	0.56	$Cs(H_2O)^-$	0.43	0.48	0.53	0.61
$Li(H_2O)_2^-$	0.52	0.57	$Cs(H_2O)_2^-$	0.44	0.50	0.64	0.73
$Li(H_2O)_3^-$	0.52	0.57	$Cs(H_2O)_3^-$	0.44	0.51	0.68	0.84
$Li(H_2O)_4^-$	0.43	0.55	$Cs(H_2O)_4^-$	0.43	0.52	0.73	0.94
$Li(H_2O)_5^-$	0.46	0.57	$Cs(H_2O)_5^-$	0.42	0.56		1.03
$Li(H_2O)_6^-$	0.44	0.63	$Cs(H_2O)_6^-$	0.42	0.57		1.08

DOI: 10.1021/jp512177j
J. Phys. Chem. A 2015, 119, 2845–2856

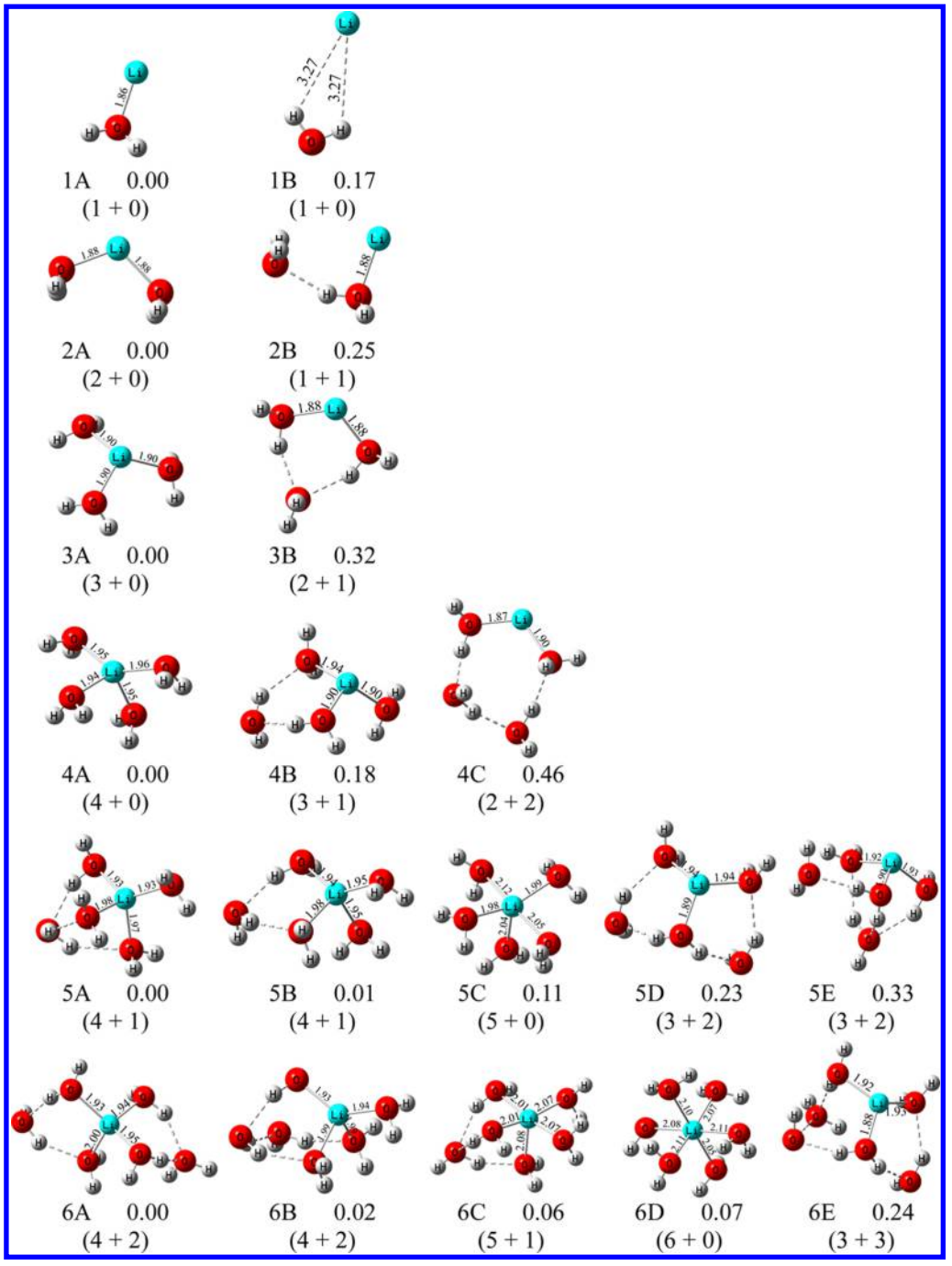

Figure 3. Geometries of the typical low-lying isomers of $Li(H_2O)_n^-$ (n = 1–6).

The most stable isomer of $Li(H_2O)_3^-$ (3A) is developed from 2A by attaching the third water molecule in the same way as the other two water molecules with Li–O bonds slightly elongated. The calculated VDE is 0.50 eV, in good agreement with the experimental result (0.57 eV). Isomer 3B has a (2 + 1) form, and its energy is significantly higher than that of 3A. Thus, the experimental feature is attributed to isomer 3A. For the neutral $Li(H_2O)_3$ cluster, the lowest lying isomer (3a) is similar to 3A with the tricoordinated hydration shell. The calculated symmetrical stretching of water molecules in neutral is 3650 cm^{-1}, in reasonable agreement with the experimental result of 3310 cm^{-1}.

In the most stable isomer of $Li(H_2O)_4^-$ (4A), the Li atom is surrounded by four water molecules and the first hydration shell is completed. The theoretical VDE (0.48 eV) fits well the experimental value (0.55 eV). Isomer 4B is derived from 3A with the fourth water molecule forming H-bonds with the inner-shell water molecules, in the form of (3 + 1). It can be directly ruled out from our experiments due to its high relative energy (0.18 eV). Thus, isomer 4A is most likely to be present in our experiments. The most stable isomer of neutral $Li(H_2O)_4$ (4a) has the tetra-coordinated geometry, analogous to that of 4A. The tri- and bicoordinated isomers are energetically unfavorable by comparing to the tetra-coordinated one. The theoretical stretching frequency of water molecules in neutral is 3592 cm^{-1}, close to observation of the 0.96 eV band in the experiments.

DOI: 10.1021/jp512177j
J. Phys. Chem. A 2015, 119, 2845–2856

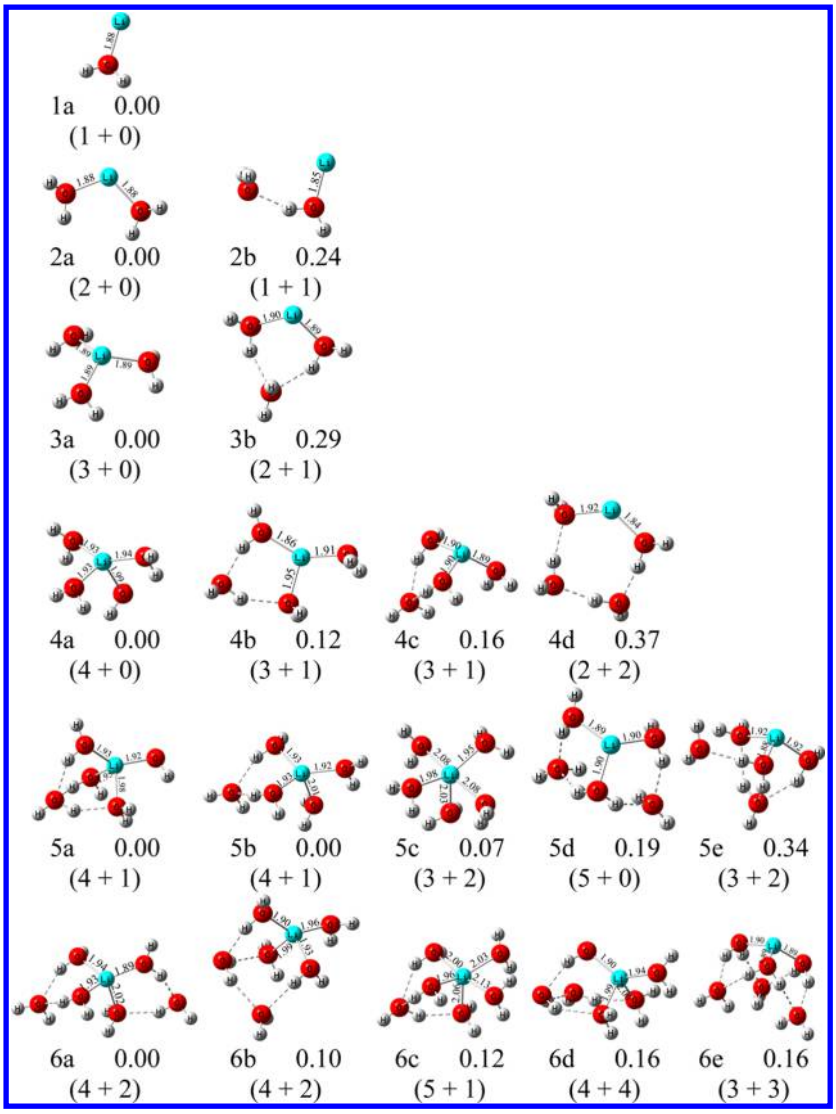

Figure 4. Geometries of the typical low-lying isomers of neutral $Li(H_2O)_n$ (n = 1−6).

The lowest lying isomer of $Li(H_2O)_5^-$ (5A) is in the form of (4 + 1) and can be viewed as developing of 4A, in which the fifth water molecule bridges three ligands of the first shell through three water−water H-bonds. The calculated VDE of isomer 5A is 0.51 eV, in good consistence with the experimental value (0.57 eV). Degenerate in energy with 5A, isomer 5B is also evolved from 4A with the fifth water molecule bridging two ligands of the first shell. Its calculated VDE (0.53 eV) also matches the experimental one (0.57 eV). Isomer 5C is penta-coordinated with longer Li−O bonds due to the space repulsive effects among adjacent water molecules. Its contribution to our experiments is low since the relative energy of isomer 5C is 0.11 eV. Isomers 5D and 5E are both tricoordinated with outer-shell water molecules at distinct positions. Their presence in the experiments can be safely ruled out by considering their much higher relative energies. Thus, isomers 5A and 5B are the most probable ones detected in our experiments. The most stable isomer of neutral $Li(H_2O)_5$ (5a) resembles the (4 + 1) structure of anionic isomer 5A but with different oriented O−H bonds. This phenomenon presents in isomer 5b with counterpart 5B. Penta-coordinated isomer 5c and tricoordinated isomer 5d are similar to 5C and 5D, respectively.

The most stable isomer of $Li(H_2O)_6^-$ (6A) evolves from 5B with the sixth water molecule forming H-bonds with the remaining ligands of the first shell. Its calculated VDE (0.43 eV) is close to that of experiments (0.63 eV). Isomer 6B is degenerate in energy with 6A, in which the sixth water molecule is bridged between the first and second shell water molecules based on isomer 5A via water−water H-bonds. Isomer 6B is in the form of (4 + 2) and its theoretical VDE (0.55 eV) is in good agreement with the experimental result (0.63 eV). Derived from 5C, isomer 6C is in the form of (5 + 1) with the sixth water molecule acting as hydrogen donor and double acceptors to the first shell water molecules. The calculated VDE (0.42 eV) of isomer 6C is also close to the experimental one (0.63 eV). Isomer 6D is approximately a hexa-coordinated octahedron without any water−water H-bonds. Its theoretical VDE (0.52 eV) is consistent with the experimental value (0.63 eV) but the corresponding relative energy is 0.07 eV. Another energetically unfavorable isomer is tricoordinated. Therefore, the spectrum of $Li(H_2O)_6^-$ is mainly attributed to isomers 6A and 6B. Isomer 6C may exist in our experiments. For the neutral $Li(H_2O)_6$ cluster, the lowest lying isomer (6a) is similar to 6A with tetra-coordination. The other low-lying isomers can

DOI: 10.1021/jp512177j
J. Phys. Chem. A 2015, 119, 2845−2856

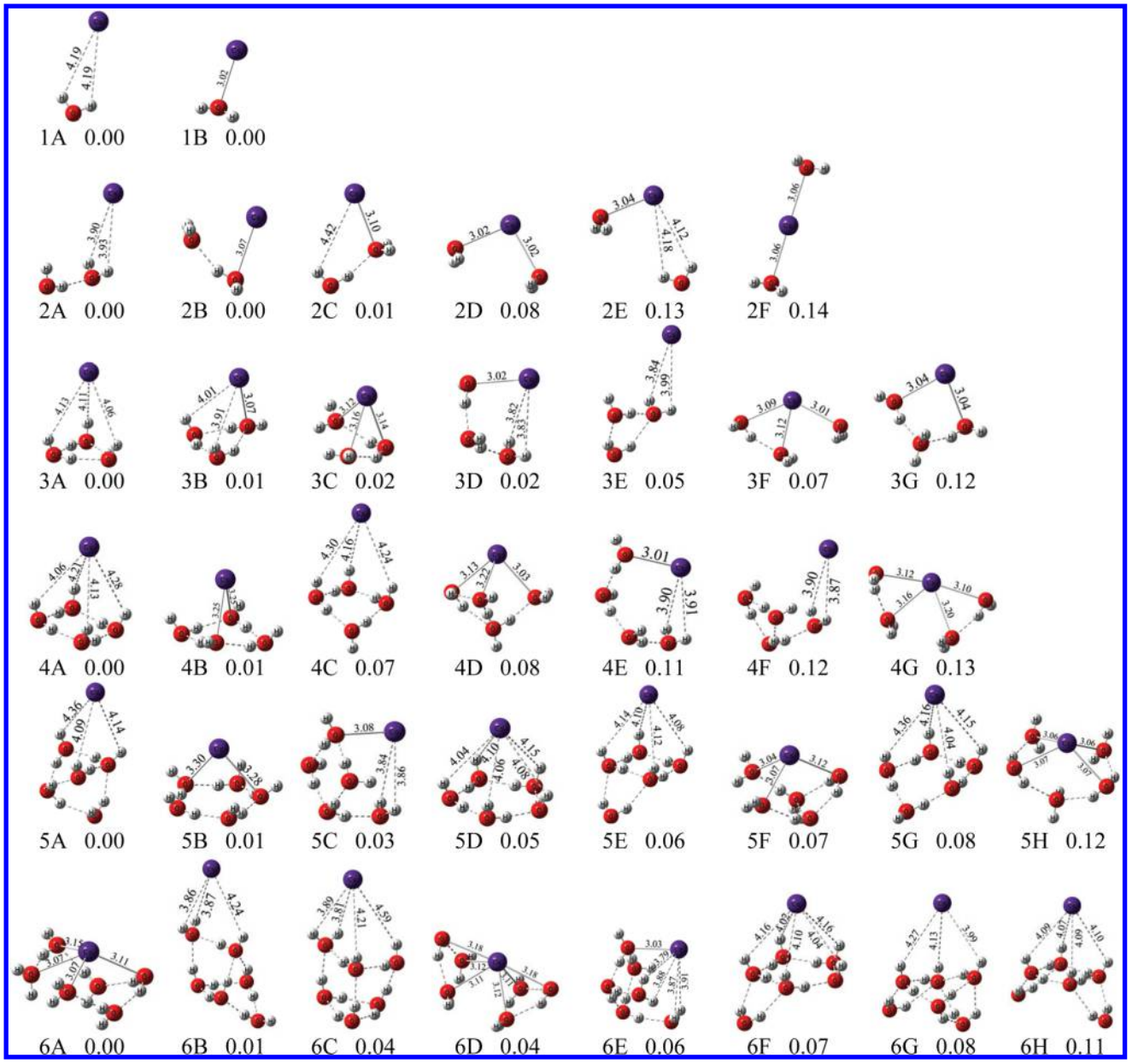

Figure 5. Geometries of the typical low-lying isomers of $Cs(H_2O)_n^-$ (n = 1−6).

be seen as evolved from the less stable neutral isomers of $Li(H_2O)_5$.

Our studies demonstrated that the most stable isomers of $Li(H_2O)_n^-$ (n = 1−6) clusters are present in our experiments. In these isomers, the Li atom is gradually and tightly surrounded by water molecules and no water−water H-bond has been formed for $n \leq 4$. The water−water H-bonds start to appear as the fifth and sixth water molecules stay at the second hydration shell. The structures of neutral $Li(H_2O)_n$ (n = 1−6) are similar to those of anions. Four water molecules are needed to close the first hydration shell of $Li^{-/0}$, consistent with the previous theoretical calculations.[34,48]

4.2. $Cs(H_2O)_n^-$ and $Cs(H_2O)_n$. The structures of $Cs(H_2O)_n^-$ and $Cs(H_2O)_n$ are flexible and therefore there are many isomers with small energy differences, especially for the clusters with $n \geq 5$.

The $Cs(H_2O)^-$ cluster favors two distinctly different isomers degenerate in energy as the global minima, namely H-end and O-end structures.[45] Isomer 1A has an H-end structure with the water molecule orienting toward the Cs atom by two H atoms. Its theoretical VDE is 0.80 eV, in reasonable agreement with the experimental measurement of feature X′ (0.61 eV). Isomer 1B exhibits an O-end structure in which the water molecule is bound to the Cs atom via its oxygen atom, analogous to $Li(H_2O)^-$. The calculated VDE (0.56 eV) is in consistence with the experimental value of feature X (0.48 eV). Both isomers 1A and 1B are most likely to be present in our experiments to contribute to the spectral features. The neutral $Cs(H_2O)$ cluster only exists as O-end configuration. The global minimum isomer (1a) is similar to 1B with slightly shortened Cs−O bond length.

For the $Cs(H_2O)_2^-$ cluster, the first two isomers 2A and 2B have identical energies and can be derived from isomers 1A and 1B, respectively. The second water molecule forms H-bond with the first one and loosely interacts with the Cs atom. The theoretical VDE (0.97 eV) of isomer 2A is in reasonable

DOI: 10.1021/jp512177j
J. Phys. Chem. A 2015, 119, 2845−2856

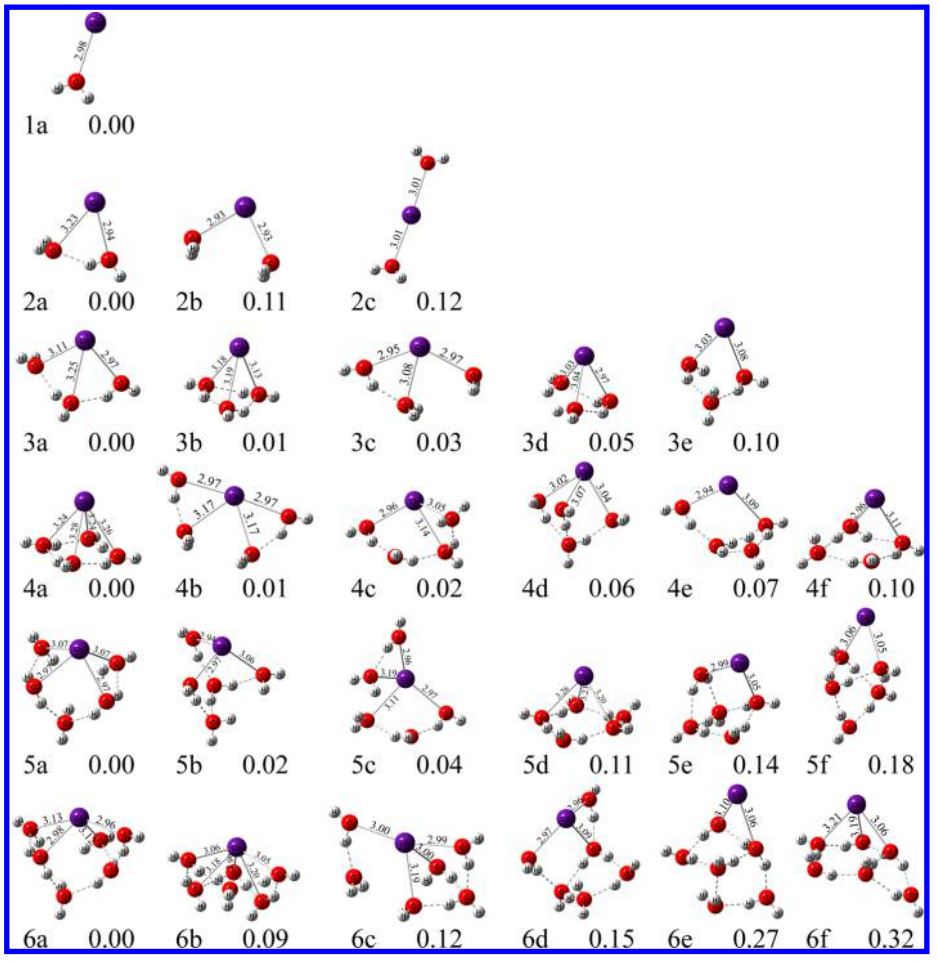

Figure 6. Geometries of the typical low-lying isomers of $Cs(H_2O)_n$ (n = 1−6).

agreement with the experimental value of feature X′ (0.73 eV) and that of isomer 2B (0.58 eV) fits well the measurement of feature X (0.50 eV). Almost degenerate in energy with the most stable isomers, isomer 2C has Cs−H and Cs−O interactions as well as one water−water H-bond. The calculated VDE (0.79 eV) of isomer 2C is in agreement with the experimental value of feature X′ (0.73 eV). In isomer 2D, two water molecules are symmetrically bound to the Cs atom via the two oxygen atoms without water−water H-bond. The calculated VDE (0.56 eV) is in accordance with the experimental result of feature X (0.50 eV) but its energy is 0.08 eV higher. The relative energies of isomers 2E and 2F are much higher and they are excluded from our experiments. Thus, isomer 2A is the probable one contributing to the feature X′ and isomer 2B is the one contributing to the feature X. Isomer 2C may also exist in our experiments. The most stable isomer of neutral $Cs(H_2O)_2$ (2a) has a water dimer binding to the Cs atom via the two oxygen atoms. Isomer 2b is similar to 2D. In isomer 2c, two water molecules linearly occupy the two opposite sides of the Cs atom.

The lowest lying isomer of $Cs(H_2O)_3^-$ (3A) is an H-end structure with the Cs atom coordinated by a $(H_2O)_3$ ring through three Cs−H interactions. Its theoretical VDE (0.98 eV) agrees well with the experimental value of feature X′ (0.84 eV). Isomer 3B is derived from 2C with two Cs−H interactions and one Cs−O band. Its calculated VDE (0.67 eV) is in reasonable accordance with the experimental results. Isomer 3C has O-end configuration with the Cs atom at the vertex of nearly tetrahedral cluster, in which there are three Cs−O bonds and two water−water H-bonds. The calculated VDE of isomer 3C is 0.61 eV, consistent with the experimental value obtained from feature X (0.51 eV). The relative energy of isomer 3D is 0.02 eV and it can be viewed as being evolved from 2E with the third water molecule bridging the first two water molecules through two H-bonds. The calculated VDE of isomer 3D is 0.67 eV, close to the experimental result. Isomer 3E is evolved from 2A with the third water molecule forming two H-bonds with the first two water molecules. Its calculated VDE (1.11 eV) is much higher than the experimental one. Isomer 3F has tricoordinated O-end geometry, in which three Cs−O bonds are almost coplanar and one water−water H-bond forms. Although the theoretical VDE (0.53 eV) of isomer 3F is in good agreement with that of feature X (0.51 eV), it has a relative energy of 0.07 eV. Therefore, isomer 3A is the most probable one contributing to the feature X′ in the spectrum of $Cs(H_2O)_3^-$ and isomer 3C is present to dedicate to the feature X. Isomers 3B and 3D may also coexist in our experiments. For the neutral $Cs(H_2O)_3$ cluster, the most stable isomer (3a) has the tricoordinated Cs atom and nonplanar ligands, in which two water−water H-bonds are formed. Degenerate in energy with 3a, isomer 3b has a $(H_2O)_3$ ring coordinating to the Cs atom through the three oxygen atoms.

The most stable isomer of $Cs(H_2O)_4^-$ (4A) is derived from 3A with the Cs atom locating above the $(H_2O)_4$ ring. Four H atoms of the four water molecules are orientated toward the Cs atom. The calculated VDE of isomer 4A is 1.06 eV, in good

DOI: 10.1021/jp512177j
J. Phys. Chem. A 2015, 119, 2845−2856

Table 2. Relative Energies of the Low Energy Isomers of $Li(H_2O)_n^-$ (n = 1−6) as Well as the Comparison of Their Theoretical ADEs and VDEs Based on CCSD(T)//M06-2X/6-311++G** to the Experimental Measurements[a]

			ADE(eV)		VDE(eV)	
	isomer	ΔE (eV)	theo.	expt.	theo.	expt.
$Li(H_2O)^-$	**1A**	0.00	0.50	0.52	0.51	0.56
	1B	0.17	0.31		0.87	
$Li(H_2O)_2^-$	**2A**	0.00	0.45	0.52	0.51	0.57
	2B	0.25	0.44		0.49	
$Li(H_2O)_3^-$	**3A**	0.00	0.50	0.52	0.50	0.57
	3B	0.32	0.47		0.46	
$Li(H_2O)_4^-$	**4A**	0.00	0.43	0.43	0.48	0.55
	4B	0.18	0.37		0.49	
	4C	0.46	0.34		0.53	
$Li(H_2O)_5^-$	**5A**	0.00	0.44	0.46	0.51	0.57
	5B	0.01	0.39	0.46	0.53	0.57
	5C	0.11	0.36		0.45	
	5D	0.23	0.45		0.56	
	5E	0.33	0.41		0.47	
$Li(H_2O)_6^-$	**6A**	0.00	0.34	0.44	0.43	0.63
	6B	0.02	0.47	0.44	0.55	0.63
	6C	0.06	0.39		0.42	
	6D	0.07	0.49		0.52	
	6E	0.24	0.39		0.55	

[a]The isomers labeled in bold are the most probable isomers in the experiments.

accordance with the experimental one of feature X′ (0.94 eV). Nearly energetically degenerate isomer 4B also has a $(H_2O)_4$ ring coordinating to Cs via two oxygen atoms with bicoordinated O-end configuration. The Cs−O bonds are elongated compared to those of 3C. The calculated VDE (0.65 eV) of isomer 4B is in good agreement with the experimental one of feature X (0.52 eV). The geometry of isomer 4C is similar to that of 4A but with three H atoms orienting toward the Cs atom and the remaining one pointing away from the Cs atom. The calculated VDE (0.96 eV) of isomer 4C is in good agreement with the experimental value of feature X′ (0.94 eV) but with the relative energy of 0.07 eV. Isomer 4D is developed from 3F with three water molecules staying at the first hydration shell through Cs−O interactions and one water molecule bridging the three ligands via three water−water H-bonds. Although its calculated VDE (0.51 eV) is in excellent agreement with the experimental value of feature X, its contribution to the feature X is low owing to its relative energy of 0.08 eV. Isomers 4E, 4F and 4G can not be present in our experiments since they are energetically unfavorable. Thus, isomer 4A is most likely to be present to contribute to the feature X′ and isomer 4B is the probable one dedicating to the feature X. In the most stable isomer of neutral $Cs(H_2O)_4$ (4a), the Cs atom is coordinated by a $(H_2O)_4$ ring through four Cs−O bonds which are elongated compared to those of isomer 3b. It has rectangular pyramid geometry with Cs locating at the vertex. Nearly degenerate in energy with 4a, isomer 4b has almost planar geometry, similar to that of 4G, in which two water dimers half surround the Cs atom.

The lowest lying isomer of $Cs(H_2O)_5^-$ (5A) is developed from H-end structure 4C with the fifth water molecule bridging two H_2O of the first and second shells through two H-bonds. The calculated VDE (1.08 eV) of isomer 5A is close to the experimental one (1.03 eV) of feature X′. Isomer 5B is

Table 3. Relative Energies of the Low Energy Isomers of $Cs(H_2O)_n^-$ (n = 1−6) as Well as the Comparison of Their Theoretical ADEs and VDEs Based on M06-2X Functional to the Experimental Measurements[a]

			ADE(eV)		VDE(eV)	
	isomer	ΔE (eV)	theo.	expt.	theo.	expt.
$Cs(H_2O)^-$	**1A**	0.00	0.53	0.53	0.80	0.61
	1B	0.00	0.53	0.43	0.56	0.48
$Cs(H_2O)_2^-$	**2A**	0.00	0.51	0.64	0.97	0.73
	2B	0.00	0.51	0.44	0.58	0.50
	2C	0.01	0.50		0.79	
	2D	0.08	0.54		0.56	
	2E	0.13	0.38		0.76	
	2F	0.14	0.51		0.55	
$Cs(H_2O)_3^-$	**3A**	0.00	0.51	0.68	0.98	0.84
	3B	0.01	0.52		0.67	
	3C	0.02	0.54	0.44	0.61	0.51
	3D	0.02	0.49		0.67	
	3E	0.05	0.55		1.11	
	3F	0.07	0.46		0.53	
	3G	0.12	0.46		0.49	
$Cs(H_2O)_4^-$	**4A**	0.00	0.52	0.73	1.06	0.94
	4B	0.01	0.53	0.43	0.65	0.52
	4C	0.07	0.45		0.96	
	4D	0.08	0.49		0.51	
	4E	0.11	0.41		0.72	
	4F	0.12	0.39		1.19	
	4G	0.13	0.39		0.54	
$Cs(H_2O)_5^-$	**5A**	0.00	0.69		1.08	1.03
	5B	0.01	0.56	0.42	0.70	0.56
	5C	0.03	0.52		0.85	
	5D	0.05	0.51		1.09	
	5E	0.06	0.64		1.20	
	5F	0.07	0.43		0.56	
	5G	0.08	0.49		1.08	
	5H	0.12	0.33		0.47	
$Cs(H_2O)_6^-$	**6A**	0.00	0.45	0.42	0.54	0.57
	6B	0.01	1.17		1.30	1.08
	6C	0.04	0.68		1.44	
	6D	0.04	0.34		0.64	
	6E	0.06	0.38		0.97	
	6F	0.07	0.70		1.25	
	6G	0.08	0.62		1.24	
	6H	0.11	0.63		1.34	

[a]The isomers labeled in bold are the most probable isomers in the experiments.

developed from 4B with a $(H_2O)_5$ ring coordinating to Cs, in which two oxygen atoms of two water molecules are bound to the Cs atom with bicoordinated O-end geometry. Its theoretical VDE (0.70 eV) agrees well with the experimental result estimated from the feature X (0.56 eV). Evolved from 4E, isomer 5C has the fifth water molecule behaving in the same way as the fourth one. Its theoretical VDE (0.85 eV) is inconsistent with the experimental value. In isomer 5D, five H atoms of the five water molecules are symmetrically headed toward the Cs atom and the remaining H atoms participate in the water−water H-bonds of a $(H_2O)_5$ ring. Its calculated VDE (1.09 eV) is in rational accordance with the experimental value of feature X′ (1.03 eV). Isomer 5E is an H-end structure and isomer 5F is an O-end structure. They are higher than isomer 5A by 0.06 and 0.07 eV respectively. Thus, the feature X of

DOI: 10.1021/jp512177j
J. Phys. Chem. A 2015, 119, 2845−2856

$Cs(H_2O)_5^-$ spectrum is mainly attributed to isomer 5B. Isomer 5A is populated in our experiments for feature X′ and isomers 5C and 5D may also be detected. The most stable isomer of neutral $Cs(H_2O)_5$ (5a) resembles 5H with tetra-coordinated O-end structure. Four Cs−O bonds are shortened compared to those in neutral 4a.

For $Cs(H_2O)_6^-$ cluster, tetra-coordinated isomer 6A can be viewed as developed from 5F with the sixth water molecule binding to the Cs atom via its oxygen atom and forming one water−water H-bond. The theoretical VDE (0.54 eV) fits well the experimental measurement of feature X (0.57 eV). Energetically degenerate isomer 6B has H-end structure with three H atoms of two water molecules pointing to the Cs atom and eight formed water−water H-bonds. Its theoretical VDE (1.30 eV) is in reasonable agreement with the experimental value of feature X′ (1.08 eV). In H-end isomer 6C, two layers of $(H_2O)_3$ clusters similar to a prism reside under the Cs atom. Its calculated VDE (1.44 eV) is far from our experimental result. In hexa-coordinated O-end isomer 6D, two water trimers symmetrically half surround the Cs atom. Its calculated VDE (0.64 eV) is close to the experimental observation of feature X (0.57 eV). The other isomers have H-end configurations and their calculated VDEs are far beyond the experimental measurement of feature X (0.57 eV). Thus, the feature X in the spectrum of $Cs(H_2O)_6^-$ is mainly dedicated by isomer 6A. Isomer 6B may be weakly populated and contributes to the feature X′. Isomer 6D may also be found in our experiments. The lowest lying isomer of neutral $Cs(H_2O)_6$ (6a) is tetra-coordinated and developed from neutral 5a by inserting the sixth water molecule between the first and second hydration shells.

Two types of anionic structures with nearly identical energies coexist and contribute to different spectral features in the spectra of $Cs(H_2O)_n^-$ clusters. The higher EBE features are mainly dedicated by the H-end structures while the lower EBE features are contributed by the O-end structures. In the H-end structures, the water molecules are oriented toward Cs by the hydrogen site, while they interact with Cs through oxygen atoms in the O-end structures. In both types of anionic structures, the water molecules also form water−water H-bonds and prefer to reside on one side of Cs with Cs sticking on the surface of the water−water H-bonds network. With increasing number of water molecules, the coordination number varies with the cluster size, which increases to four with n up to 4 and decreases to three at n = 5 and 6 in the H-end structures; while increases to three with n up to 3 and decreases to two at n = 4 and 5, then increases to four again at n = 6 for the O-end structures. In the neutral $Cs(H_2O)_n$ clusters, there is only O-end type of structure, in which the O atoms of water molecules interact with Cs and H atoms participate in water−water H-bonds. The water−water H-bonds network also locates on one side of Cs and the coordination number of the Cs atom is 4.

4.3. Discussion. The anionic and neutral $Li(H_2O)_n$ clusters share similar structures and both prefer inner geometries with the Li atom being surrounded by water molecules. The maximum Li−O bonds without water−water H-bonds are formed for $n \leq 4$ because the interaction between the Li atom and water molecule is stronger than water−water H-bonds. The Li atom accommodates up to four water molecules in its first hydration shell and additional water molecules occupy the second hydration shell through water−water H-bonds. These corresponding anionic and neutral structures are in accordance with the previous theoretical calculations.[34,45,48]

Two classes of structures coexist for the anionic $Cs(H_2O)_n^-$ clusters in our experiments, namely H-end and O-end structures.[45] The VDEs of O-end structures are lower than those of H-end structures and the O-end structures become more favored than the H-end ones when the number of water molecules increases. Both types of structures have the Cs atom locating on the surface of water−water H-bonds network and are nearly energetically degenerate. In the H-end structures with the H atoms of water molecules orienting toward the Cs atom, the maximum number of coordinated water molecules is four as $n \leq 4$. For the larger cluster anions (n = 5 and 6), the Cs atom is hydrated by only three H atoms since Cs−H interactions are weaker than water−water H-bonds. In the O-end structures with the O atoms of water molecules interacting with Cs, there are no more than three water molecules directly bound to Cs in the first hydration shell for $n \leq 5$ because the Cs−O bond is weaker than water−water H-bonds. At n = 6, the coordination number changes to 4 due to the stabilization of cluster by both Cs−O interactions and water−water H-bonds. For the neutral $Cs(H_2O)_n$ clusters, only the O-end structures exist. The Cs atom also sticks on the surface of water−water H-bonds network and four water molecules form the first hydration shell of the Cs atom. The spectral shift of the weak peak dedicated by the H-end isomers is similar to that of $Na(H_2O)_n^-$,[27] in which the observed photoelectron bands are mainly due to the isomers with Na−H interactions. The H-end structures of $Cs(H_2O)_5^-$ and $Cs(H_2O)_6^-$ are different from those of $Na(H_2O)_5^-$ and $Na(H_2O)_6^-$,[45] which are analogous to 5G and 6C, respectively, while in the smaller cluster anions, their difference is modest. Otherwise, the structures of neutral $Cs(H_2O)_{1-3}$ are in good agreement with those calculated by Sudolská et al.[67]

The structures and geometrical evolutions of $Cs(H_2O)_n^{-/0}$ are distinct from those of $Li(H_2O)_n^{-/0}$. The Li atom prefers to be surrounded by water molecules without water−water H-bonds in the first hydration shell, while the Cs atom cannot be surrounded by water molecules and stays on the surface of water−water H-bonds network. This can be ascribed to the larger atomic radius and smaller surface charge density of the Cs atom which provide large space for forming stronger water−water H-bonds compared to the Cs−H or Cs−O interactions.

It is worth mentioning that the peak at 1.90 eV in the 532 nm spectrum of $Li(H_2O)^-$ is due to the transition from the anionic ground state (^{1}S) to the neutral first excited state (^{2}P). The VDE of the same transition from the Li^- ground state (^{1}S) to the first excited state of Li atom (^{2}P) is about 2.47 eV,[49] which can be confirmed by the nearly degenerate energy levels ($^2P^o_{1/2}$ and $^2P^o_{3/2}$) of Li atom at 1.85 eV.[68] That peak shifts toward lower EBE (1.90 eV) upon addition of the first water molecule because the increased stability for the neutral is larger than the corresponding anion when a water molecule is connected to the $Li^{0/-}$. Similarly, that peak shifts toward lower EBE side with increasing number of water molecules from $Li(H_2O)^-$ to $Li(H_2O)_4^-$. For $Li(H_2O)_5^-$ and $Li(H_2O)_6^-$, the fifth and sixth water molecules do not interact directly with the Li atom, thus, the excited state peak shifts toward higher EBE in the same manner as the peak of the ground state. This finding is in agreement with the results of Takasu et al.[49] In the 532 nm spectrum of Cs^-, the second and third peaks at 1.86 and 1.93 eV correspond to the transitions from anionic ground state (^{1}S) to the first excited state ($^2P^o_{1/2}$) and second excited state ($^2P^o_{3/2}$) respectively, which can be verified from the first and second excited energy levels of neutral cesium at 1.39[69] and

DOI: 10.1021/jp512177j
J. Phys. Chem. A 2015, 119, 2845−2856

1.45[70] respectively. These peaks shift to the VDEs of 1.51 and 1.77 eV for $Cs(H_2O)^-$. These peaks of $Cs(H_2O)_n^-$ shift toward lower EBE and become broader with increasing number of water molecules similarly to the case of $Li(H_2O)_n^-$. To verify those peaks theoretically, we calculated the VDEs from the Li^-, $Li(H_2O)^-$, Cs^-, and $Cs(H_2O)^-$ anions to the excited states of their neutral counterparts using TDDFT[71,72] method with the M06-2X functional and the same basis sets as optimizations. The VDE of $Li(^2P)$-$Li^-(^1S)$ transition is calculated to be ~2.57 eV, close to the experimental value of 2.47 eV. The VDE of $Li(H_2O)^-$ for the $Li(^2P)$-$Li^-(^1S)$ transition is calculated to be 2.00 eV, which shifts toward lower EBE compared to that of Li^- and is also in agreement with the experimental value of 1.90 eV. The VDEs of $Cs(^2P^o_{1/2})$−$Cs^-(^1S)$ and $Cs(7^2S_{1/2})$−$Cs^-(6^1S)$ transitions are calculated to be 1.81 and 2.48 eV, close to the experimental values of $(^2P^o_{1/2})$ 1.86, $(^2P^o_{3/2})$ 1.93 and $(7^2S_{1/2})$ 2.77 eV. The theoretical VDEs of the transitions from the $Cs(H_2O)^-$ anion (1B) ground state to the excited states of its neutral are calculated to be 1.65 and 1.85 eV by the TDDFT method, consistent with the experimental features at 1.51 and 1.77 eV.

5. CONCLUSIONS

We conducted photoelectron spectroscopy experimental measurements and *ab initio* calculations on the $Li(H_2O)_n^-$ and $Cs(H_2O)_n^-$ (n = 0−6) clusters to investigate the coordination nature and structural evolution of the Li and Cs atoms in water. In both anionic and neutral clusters, the Li atom tends to be surrounded by water molecules through Li−O interactions without any water−water H-bond in the first hydration shell, while the Cs atom sticks on the surface of water−water H-bonds network. The first hydration shells of Li in its anionic and neutral states are both completed at n = 4. For the $Cs(H_2O)_n^-$ clusters, two types of structures, H-end and O-end, were identified. They are nearly degenerate in energy. The coordination numbers of Cs in both the H-end and O-end structures vary with the number of water molecules. For the $Cs(H_2O)_n$ clusters, only the O-end structures exist and four water molecules stay within the first hydration shell. These results show that the structures of the alkali-water clusters are determined by the delicate balance between multiple forces as well as the effect of excess electron, which may provide general information for the hydration process of alkali atoms as well as the study of solvated electron pair.

■ ASSOCIATED CONTENT

Supporting Information

Relative energies, ADEs and VDEs of the low-lying isomers of $Li(H_2O)_n^-$ (n = 1−6) and $Cs(H_2O)_n^-$ (n = 1−6) as well as the detailed geometries of them and their neutral counterparts calculated by using the M06-2X functional and the same basis sets as optimizations. This material is available free of charge via the Internet at http://pubs.acs.org.

■ AUTHOR INFORMATION

Corresponding Authors

*(W.-J.Z.) E-mail: zhengwj@iccas.ac.cn. Telephone: +86 10 62635054. Fax: +86 10 62563167.

*(Y.Q.G.) E-mail: gaoyq@pku.edu.cn.

Notes

The authors declare no competing financial interest.

■ ACKNOWLEDGMENTS

This work was supported by the Knowledge Innovation Program of the Chinese Academy of Sciences (Grant No. KJCX2-EW-H01), the Natural Science Foundation of China (Grant No. 21403249 to G.F. and 91027044 to Y.Q.G), and the National Key Basic Research Foundation of China (2012CB917304 to Y.Q.G.). The theoretical calculations were conducted on the ScGrid and DeepComp 7000 of the Supercomputing Center, Computer Network Information Center of Chinese Academy of Sciences.

■ REFERENCES

(1) Dzidic, I.; Kebarle, P. Hydration of the Alkali Ions in the Gas Phase. Enthalpies and Entropies of Reactions $M^+(H_2O)_{n-1} + H_2O = M^+(H_2O)_n$. *J. Phys. Chem.* **1970**, *74*, 1466−1474.

(2) Dalleska, N. F.; Tjelta, B. L.; Armentrout, P. B. Sequential Bond Energies of Water to Na^+ ($3s^0$), Mg^+ ($3s^1$), and Al^+ ($3s^2$). *J. Phys. Chem.* **1994**, *98*, 4191−4195.

(3) Rodgers, M. T.; Armentrout, P. B. Collision-Induced Dissociation Measurements on $Li^+(H_2O)_n$, n = 1−6: The First Direct Measurement of the Li^+−OH_2 Bond Energy. *J. Phys. Chem. A* **1997**, *101*, 1238−1249.

(4) Weinheimer, C. J.; Lisy, J. M. Vibrational Predissociation Spectroscopy of $Cs^+(H_2O)_{1-5}$. *J. Chem. Phys.* **1996**, *105*, 2938−2941.

(5) Vaden, T. D.; Lisy, J. M.; Carnegie, P. D.; Dinesh Pillai, E.; Duncan, M. A. Infrared Spectroscopy of the $Li^+(H_2O)$Ar Complex: The Role of Internal Energy and Its Dependence on Ion Preparation. *Phys. Chem. Chem. Phys.* **2006**, *8*, 3078−3082.

(6) Miller, D. J.; Lisy, J. M. Hydrated Alkali-Metal Cations: Infrared Spectroscopy and Ab Initio Calculations of $M^+(H_2O)_{x=2-5}$Ar Cluster Ions for M = Li, Na, K, and Cs. *J. Am. Chem. Soc.* **2008**, *130*, 15381−15392.

(7) Beck, J. P.; Lisy, J. M. Infrared Spectroscopy of Hydrated Alkali Metal Cations: Evidence of Multiple Photon Absorption. *J. Chem. Phys.* **2011**, *135*, 044302.

(8) Rodriguez, O.; Lisy, J. M. Revisiting $Li^+(H_2O)_{3-4}Ar_1$ Clusters: Evidence of High-Energy Conformers from Infrared Spectra. *J. Phys. Chem. Lett.* **2011**, *2*, 1444−1448.

(9) Ke, H.; van der Linde, C.; Lisy, J. M. Insights Into Gas-Phase Structural Conformers of Hydrated Rubidium and Cesium Cations, $M^+(H_2O)_n$Ar (M = Rb, Cs; n = 3−5), Using Infrared Photodissociation Spectroscopy. *J. Phys. Chem. A* **2014**, *118*, 1363−1373.

(10) Feller, D.; Glendening, E. D.; Kendall, R. A.; Peterson, K. A. An Extended Basis Set Abinitio Study of $Li^+(H_2O)_n$, n = 1−6. *J. Chem. Phys.* **1994**, *100*, 4981−4997.

(11) Kim, J.; Lee, S.; Cho, S. J.; Mhin, B. J.; Kim, K. S. Structures, Energetics, and Spectra of Aqua−Sodium(I): Thermodynamic Effects and Nonadditive Interactions. *J. Chem. Phys.* **1995**, *102*, 839−849.

(12) Glendening, E. D.; Feller, D. Cation-Water Interactions: The $M^+(H_2O)_n$ Clusters for Alkali Metals, M = Li, Na, K, Rb, and Cs. *J. Phys. Chem.* **1995**, *99*, 3060−3067.

(13) Wójcik, M. J.; Mains, G. J.; Devlin, J. P. Theoretical Study of $[Li(H_2O)_n]^+$ and $[K(H_2O)_n]^+$ (n = 1−4) Complexes. *Int. J. Quantum Chem.* **1995**, *53*, 49−56.

(14) Feller, D.; Glendening, E. D.; Woon, D. E.; Feyereisen, M. W. An Extended Basis Set Ab Initio Study of Alkali Metal Cation−Water Clusters. *J. Chem. Phys.* **1995**, *103*, 3526−3542.

(15) Lee, H. M.; Kim, J.; Lee, S.; Mhin, B. J.; Kim, K. S. Aqua−Potassium(I) Complexes: Ab Initio Study. *J. Chem. Phys.* **1999**, *111*, 3995−4004.

(16) Trachtman, M.; Markham, G. D.; Glusker, J. P.; George, P.; Bock, C. W. Interactions of Metal Ions with Water: Ab Initio Molecular Orbital Studies of Structure, Vibrational Frequencies, Charge Distributions, Bonding Enthalpies, and Deprotonation Enthalpies. 2. Monohydroxides. *Inorg. Chem.* **2001**, *40*, 4230−4241.

(17) Loeffler, H. H.; Rode, B. M. The Hydration Structure of the Lithium Ion. *J. Chem. Phys.* **2002**, *117*, 110−117.

DOI: 10.1021/jp512177j
J. Phys. Chem. A 2015, 119, 2845−2856

(18) Egorov, A. V.; Komolkin, A. V.; Chizhik, V. I.; Yushmanov, P. V.; Lyubartsev, A. P.; Laaksonen, A. Temperature and Concentration Effects on Li^+-Ion Hydration: A Molecular Dynamics Simulation Study. *J. Phys. Chem. B* **2003**, *107*, 3234−3242.
(19) Park, J.; Kołaski, M.; Lee, H. M.; Kim, K. S. Insights Into the Structures, Energetics, and Vibrations of Aqua−Rubidium(I) Complexes: Ab Initio Study. *J. Chem. Phys.* **2004**, *121*, 3108−3116.
(20) González, B. S.; Hernández-Rojas, J.; Wales, D. J. Global Minima and Energetics of $Li^+(H_2O)_n$ and $Ca^{2+}(H_2O)_n$ Clusters for $n \leq 20$. *Chem. Phys. Lett.* **2005**, *412*, 23−28.
(21) Bock, C.; Markham, G.; Katz, A.; Glusker, J. The Arrangement of First- and Second-Shell Water Molecules Around Metal Ions: Effects of Charge and Size. *Theor. Chem. Acc.* **2006**, *115*, 100−112.
(22) Ali, S. M.; De, S.; Maity, D. K. Microhydration of Cs^+ Ion: A Density Functional Theory Study on Cs^+−$(H_2O)_n$ Clusters (n = 1−10). *J. Chem. Phys.* **2007**, *127*, 044303.
(23) Schulz, C. P.; Haugstätter, R.; Tittes, H. U.; Hertel, I. V. Free Sodium-Water Clusters. *Phys. Rev. Lett.* **1986**, *57*, 1703−1706.
(24) Schulz, C. P.; Haugstätter, R.; Tittes, H. U.; Hertel, I. V. Free Sodium-Water Clusters: Photoionisation Studies in a Pulsed Molecular Beam Source. *Z. Phys. D: At., Mol. Clusters* **1988**, *10*, 279−290.
(25) Hertel, I. V.; Hüglin, C.; Nitsch, C.; Schulz, C. P. Photoionization of $Na(NH_3)_n$ and $Na(H_2O)_n$ Clusters: A Step Towards the Liquid Phase? *Phys. Rev. Lett.* **1991**, *67*, 1767−1770.
(26) Misaizu, F.; Tsukamoto, K.; Sanekata, M.; Fuke, K. Photoionization of Clusters of Cs Atoms Solvated with H_2O, NH_3 and CH_3CN. *Chem. Phys. Lett.* **1992**, *188*, 241−246.
(27) Takasu, R.; Misaizu, F.; Hashimoto, K.; Fuke, K. Microscopic Solvation Process of Alkali Atoms in Finite Clusters: Photoelectron and Photoionization Studies of $M(NH_3)_n$ and $M(H_2O)_n$ (M = Li, Li^-, Na^-). *J. Phys. Chem. A* **1997**, *101*, 3078−3087.
(28) Coe, J. V.; Lee, G. H.; Eaton, J. G.; Arnold, S. T.; Sarkas, H. W.; Bowen, K. H.; Ludewigt, C.; et al. Photoelectron Spectroscopy of Hydrated Electron Cluster Anions, $(H_2O)_{n=2-69}^-$. *J. Chem. Phys.* **1990**, *92*, 3980−3982.
(29) Barnett, R. N.; Landman, U. Hydration of Sodium in Water Clusters. *Phys. Rev. Lett.* **1993**, *70*, 1775−1778.
(30) Hashimoto, K.; He, S.; Morokuma, K. Structures, Stabilities and Ionization Potentials of $Na(H_2O)_n$ and $Na(NH_3)_n$ (n = 1−6) clusters. An Ab Initio MO Study. *Chem. Phys. Lett.* **1993**, *206*, 297−304.
(31) Stampfli, P.; Bennemann, K. H. Theory for the Solvation of Alkali Metal Atoms in Clusters of Polar Molecules. Many-Body Polarization Interactions. *Comput. Mater. Sci.* **1994**, *2*, 578−584.
(32) Hashimoto, K.; Morokuma, K. Ab Initio Theoretical Study of 'Surface' and 'Interior' Structures of the $Na(H_2O)_4$ Cluster and Its Cation. *Chem. Phys. Lett.* **1994**, *223*, 423−430.
(33) Hashimoto, K.; Morokuma, K. Ab Initio Molecular Orbital Study of $Na(H_2O)_n$ (n = 1−6) Clusters and Their Ions. Comparison of Electronic Structure of the "Surface" and "Interior" Complexes. *J. Am. Chem. Soc.* **1994**, *116*, 11436−11443.
(34) Hashimoto, K.; Kamimoto, T. Theoretical Study of Microscopic Solvation of Lithium in Water Clusters: Neutral and Cationic $Li(H_2O)_n$ (n = 1−6 and 8). *J. Am. Chem. Soc.* **1998**, *120*, 3560−3570.
(35) Tsurusawa, T.; Iwata, S. Theoretical Studies of Structures and Ionization Threshold Energies of Water Cluster Complexes with A Group 1 Metal, $M(H_2O)_n$ (M = Li and Na). *J. Phys. Chem. A* **1999**, *103*, 6134−6141.
(36) Tsurusawa, T.; Iwata, S. Electron-Hydrogen Bonds and OH Harmonic Frequency Shifts in Water Cluster Complexes with A Group 1 Metal Atom, $M(H_2O)_n$ (M = Li and Na). *J. Chem. Phys.* **2000**, *112*, 5705−5710.
(37) Gao, B.; Liu, Z.-F. Ionization Induced Relaxation in Solvation Structure: A Comparison Between $Na(H_2O)_n$ and $Na(NH_3)_n$. *J. Chem. Phys.* **2007**, *126*, 084501.
(38) Hashimoto, K.; Daigoku, K. Ground and Low-Lying Excited States of $Na(NH_3)_n$ and $Na(H_2O)_n$ Clusters: Formation and Localization of Solvated Electron. *Chem. Phys. Lett.* **2009**, *469*, 62−67.
(39) Hashimoto, K.; Daigoku, K. Formation and Localization of A Solvated Electron in Ground and Low-Lying Excited States of $Li(NH_3)_n$ and $Li(H_2O)_n$ Clusters: A Comparison with $Na(NH_3)_n$ and $Na(H_2O)_n$. *Phys. Chem. Chem. Phys.* **2009**, *11*, 9391−9400.
(40) Pratihar, S.; Chandra, A. Excess Electron and Lithium Atom Solvation in Water Clusters at Finite Temperature: An Ab Initio Molecular Dynamics Study of the Structural, Spectral, and Dynamical Behavior of $(H_2O)_6^-$ and $Li(H_2O)_6$. *J. Phys. Chem. A* **2010**, *114*, 11869−11878.
(41) Müller, J. P.; Zhavoronkov, N.; Hertel, I. V.; Schulz, C. P. Time-Resolved Excited State Energetics of the Solvated Electron in Sodium-Doped Water Clusters. *J. Phys. Chem. A* **2014**, *118*, 8517−8524.
(42) Alizadeh, E.; Sanche, L. Precursors of Solvated Electrons in Radiobiological Physics and Chemistry. *Chem. Rev.* **2012**, *112*, 5578−5602.
(43) Gu, J.; Leszczynski, J.; Schaefer, H. F. Interactions of Electrons with Bare and Hydrated Biomolecules: From Nucleic Acid Bases to DNA Segments. *Chem. Rev.* **2012**, *112*, 5603−5640.
(44) Simons, J. How Do Low-Energy (0.1−2 eV) Electrons Cause DNA-Strand Breaks? *Acc. Chem. Res.* **2006**, *39*, 772−779.
(45) Zhang, H.; Liu, Z.-F. The Identification of A Solvated Electron Pair in the Gaseous Clusters of $Na^-(H_2O)_n$ and $Li^-(H_2O)_n$. *J. Chem. Phys.* **2011**, *135*, 064309.
(46) Hashimoto, K.; Kamimoto, T.; Fuke, K. Ab Initio MO Study of Solvated Negative Alkali Atom Clusters: $[M(H_2O)_n]^-$ and $[M(NH_3)_n]^-$ (M = Na and Li, n = 1−3). *Chem. Phys. Lett.* **1997**, *266*, 7−15.
(47) Hashimoto, K.; Kamimoto, T.; Daigoku, K. Theoretical Study of $[Na(H_2O)_n]^-$ (n = 1−4) Clusters: Geometries, Vertical Detachment Energies, and IR Spectra. *J. Phys. Chem. A* **2000**, *104*, 3299−3307.
(48) Hashimoto, K.; Daigoku, K.; Kamimoto, T.; Shimosato, T. Microscopic Solvation and Spontaneous Ionization of Li in Small Polar Solvent Clusters: Theoretical Analysis of Photoelectron Spectra for $Li^-(H_2O)_n$ (n = 1−4). *Internet. Electron. J. Mol. Des* **2002**, *1*, 503−526.
(49) Takasu, R.; Taguchi, T.; Hashimoto, K.; Fuke, K. Microscopic Solvation Process of Single Li Atom in Small Water Clusters. *Chem. Phys. Lett.* **1998**, *290*, 481−487.
(50) Takasu, R.; Nishikawa, K.; Miura, N.; Sabu, A.; Hashimoto, K.; Schulz, C. P.; Hertel, I. V.; et al. Photodissociation Spectroscopy of Li−H_2O and Li−D_2O Complexes. *J. Phys. Chem. A* **2001**, *105*, 6602−6608.
(51) Steinbach, C.; Buck, U. Vibrational Spectroscopy of Size-Selected Sodium-Doped Water Clusters. *J. Phys. Chem. A* **2005**, *110*, 3128−3131.
(52) Buck, U.; Dauster, I.; Gao, B.; Liu, Z.-f. Infrared Spectroscopy of Small Sodium-Doped Water Clusters: Interaction with the Solvated Electron. *J. Phys. Chem. A* **2007**, *111*, 12355−12362.
(53) Zeuch, T.; Buck, U. Sodium Doped Hydrogen Bonded Clusters: Solvated Electrons and Size Selection. *Chem. Phys. Lett.* **2013**, *579*, 1−10.
(54) Xu, H.-G.; Zhang, Z.-G.; Feng, Y.; Yuan, J.; Zhao, Y.; Zheng, W. Vanadium-Doped Small Silicon Clusters: Photoelectron Spectroscopy and Density-Functional Calculations. *Chem. Phys. Lett.* **2010**, *487*, 204−208.
(55) Frisch, M. J.; Trucks, G. W.; Schlegel, H. B.; Scuseria, G. E.; Robb, M. A.; Cheeseman, J. R.; Scalmani, G.; et al. *Gaussian 09*, Revision A.02. Gaussian, Inc.: Wallingford CT, 2009.
(56) Zhao, Y.; Truhlar, D. G. Comparative DFT Study of van der Waals Complexes: Rare-Gas Dimers, Alkaline-Earth Dimers, Zinc Dimer, and Zinc-Rare-Gas Dimers. *J. Phys. Chem. A* **2006**, *110*, 5121−5129.
(57) Rappoport, D.; Furche, F. Property-Optimized Gaussian Basis Sets for Molecular Response Calculations. *J. Chem. Phys.* **2010**, *133*, 134105.
(58) Schuchardt, K. L.; Didier, B. T.; Elsethagen, T.; Sun, L.; Gurumoorthi, V.; Chase, J.; Li, J.; et al. Basis Set Exchange: A Ccommunity Database for Computational Sciences. *J. Chem. Inf. Model.* **2007**, *47*, 1045−1052.
(59) Pople, J. A.; Head-Gordon, M.; Raghavachari, K. Quadratic configuration interaction. A General Technique for Determining Electron Correlation Energies. *J. Chem. Phys.* **1987**, *87*, 5968−5975.

DOI: 10.1021/jp512177j
J. Phys. Chem. A 2015, 119, 2845−2856

(60) Tawada, Y.; Tsuneda, T.; Yanagisawa, S.; Yanai, T.; Hirao, K. A Long-Range-Corrected Time-Dependent Density Functional Theory. *J. Chem. Phys.* **2004**, *120*, 8425−8433.
(61) Vydrov, O. A.; Heyd, J.; Krukau, A. V.; Scuseria, G. E. Importance of Short-Range Versus Long-Range Hartree-Fock Exchange for the Performance of Hybrid Density Functionals. *J. Chem. Phys.* **2006**, *125*, 074106.
(62) Vydrov, O. A.; Scuseria, G. E.; Perdew, J. P. Tests of Functionals for Systems with Fractional Electron Number. *J. Chem. Phys.* **2007**, *126*, 154109.
(63) Vydrov, O. A.; Scuseria, G. E. Assessment of A Long-Range Corrected Hybrid Functional. *J. Chem. Phys.* **2006**, *125*, 234109.
(64) Chai, J.-D.; Head-Gordon, M. Long-Range Corrected Hybrid Density Functionals with Damped Aatom-Atom Dispersion Corrections. *Phys. Chem. Chem. Phys.* **2008**, *10*, 6615−6620.
(65) Haeffler, G.; Hanstorp, D.; Kiyan, I.; Klinkmüller, A. E.; Ljungblad, U.; Pegg, D. J. Electron Affinity of Li: A State-Selective Measurement. *Phys. Rev. A* **1996**, *53*, 4127−4131.
(66) Kasdan, A.; Lineberger, W. C. Alkali-Metal Negative Ions. II. Laser Photoelectron Spectrometry. *Phys. Rev. A* **1974**, *10*, 1658−1664.
(67) Sudolská, M.; Cantrel, L.; Černušák, I. Microhydration of Caesium Compounds: Cs, CsOH, CsI and Cs_2I_2 Complexes with One to Three H_2O Molecules of Nuclear Safety Interest. *J. Mol. Model.* **2014**, *20*, 1−15.
(68) Radziemski, L. J.; Engleman, R.; Brault, J. W. Fourier-Transform-Spectroscopy Measurements in the Spectra of Neutral Lithium, ^{6}Li and ^{7}Li (Li I). *Phys. Rev. A* **1995**, *52*, 4462−4470.
(69) Weber, K. H.; Sansonetti, C. J. Accurate Energies of *nS*, *nP*, *nD*, *nF*, and *nG* Levels of Neutral Cesium. *Phys. Rev. A* **1987**, *35*, 4650−4660.
(70) Eriksson, K. B. S.; Wenåker, I. New Wavelength Measurements in Cs I. *Phys. Scr.* **1970**, *1*, 21.
(71) van Leeuwen, R. Causality and Symmetry in Time-Dependent Density-Functional Theory. *Phys. Rev. Lett.* **1998**, *80*, 1280−1283.
(72) Runge, E.; Gross, E. K. U. Density-Functional Theory for Time-Dependent Systems. *Phys. Rev. Lett.* **1984**, *52*, 997−1000.

DOI: 10.1021/jp512177j
J. Phys. Chem. A 2015, 119, 2845−2856